Wind Response Control of Building with Variable Stiffness Tuned Mass Damper Using Empirical Mode Decomposition/ Hilbert Transform

Nadathur Varadarajan[1] and Satish Nagarajaiah, M.ASCE[2]

Abstract: The effectiveness of a novel semiactive variable stiffness-tuned mass damper (SAIVS-TMD) for the response control of a wind-excited tall benchmark building is investigated in this study. The benchmark building considered is a proposed 76-story concrete office tower in Melbourne, Australia. It is a slender building 306 m tall with a height to width ratio of 7.3; hence, it is wind sensitive. Across wind load data from wind tunnel tests are used in the present study. The objective of this study is to evaluate the new SAIVS-TMD system, that has the distinct advantage of continuously retuning its frequency due to real time control and is robust to changes in building stiffness and damping. In comparison, the passive tuned mass damper (TMD) can only be tuned to a fixed frequency. A time varying analytical model of the tall building with the SAIVS-TMD is developed. The frequency tuning of the SAIVS-TMD is achieved based on empirical mode decomposition and Hilbert transform instantaneous frequency algorithm developed by the writers. It is shown that the SAIVS-TMD can reduce the structural response substantially, when compared to the uncontrolled case, and it can reduce the response further when compared to the case with TMD. Additionally, it is shown the SAIVS-TMD reduces response even when the building stiffness changes by $\pm 15\%$ and is robust; whereas, the TMD loses its effectiveness under such building stiffness variations. It is also shown that SAIVS-TMD can reduce the response similar to an active TMD; however, with an order of magnitude less power consumption.

DOI: 10.1061/(ASCE)0733-9399(2004)130:4(451)

CE Database subject headings: Wind loads; Damping; Structural control; Stiffness; Buildings, high-rise; Australia.

Introduction

The effectiveness of tuned mass dampers (TMDs) (Den Hartog 1947) and multiple tuned mass dampers (Igusa and Xu 1992) have been investigated. TMD is very sensitive to tuning frequency ratio, even when optimally designed (Den Hartog 1947). MTMD (Igusa and Xu 1992; Abe and Fujino 1994; Kareem and Klein 1995) can overcome the limitation of the TMD by distributing the natural frequencies of a number of TMDs around the fundamental natural frequency of the structure. Active tuned mass dampers (ATMDs) (Soong 1990; Spencer and Nagarajaiah 2003; Yang et al. 2004) and active mass dampers (Soong 1990; Reinhorn et al. 1993; Ikeda et al. 2001; Spencer and Nagarajaiah 2003) have also been developed and implemented widely for the active response control of buildings and bridges. Semiactive TMD has been investigated by Hrovat et al. (1983) and Abe and Igusa (1996).

Semiactive control of linear and nonlinear structures has gained considerable attention in recent years (Spencer and Nagarajaiah 2003). In semiactive systems reactive forces that develop due to variable stiffness or damping devices in the system control the response, as compared to direct application of active control force. Devices which can vary stiffness or damping need nominal power. Additionally, semiactive systems can behave as passive devices in the event of a loss of power; thus are reliable. Several new variable damping devices, such as magnetorheological dampers (Spencer et al. 1997), variable orifice dampers (Kurata et al. 1999; Symans and Constantinou 1999), electrorheological dampers (Gavin 1998), and variable stiffness devices have been developed (Kobori and Takahashi 1993; Bobrow et al. 2000; Yang et al. 2000; Nasu et al. 2001). A new semiactive continuously and independently variable stiffness (SAIVS) device has been developed and patented by Nagarajaiah [U.S. Patent No. 6,098,969 (2000)]. Based on this device a new semiactive variable stiffness-tuned mass damper (SAIVS-TMD) has been developed by Nagarajaiah and Varadarajan (2000). The SAIVS-TMD has a single mass with a variable stiffness spring as shown in Fig. 1. The system has the distinct advantage of continuously retuning its frequency due to real time control thus making it robust to changes in building stiffness and damping; whereas, the passive TMD can only be tuned to a fixed frequency. In addition, SAIVS-TMD will behave as a fail-safe TMD system; hence, SAIVS-TMD is reliable.

In this study, the effectiveness of the new SAIVS-TMD for the vibration control of a wind-excited tall benchmark building is evaluated. An analytical model of the tall building with the SAIVS-TMD is developed. The frequency tuning of the SAIVS-TMD is achieved based on a new empirical mode decomposition (EMD) and Hilbert transform (HT) instantaneous frequency con-

[1]Graduate Student, Dept. of Civil and Environmental Engineering, MS 318, Rice Univ., Houston, TX 77005.

[2]Associate Professor, Dept. of Civil and Environmental Engineering, MS 318, Rice Univ., Houston, TX 77005.

Note. Associate Editor: Bill F. Spencer Jr. Discussion open until September 1, 2004. Separate discussions must be submitted for individual papers. To extend the closing date by one month, a written request must be filed with the ASCE Managing Editor. The manuscript for this paper was submitted for review and possible publication on March 5, 2003; approved on March 5, 2003. This paper is part of the ***Journal of Engineering Mechanics***, Vol. 130, No. 4, April 1, 2004. ©ASCE, ISSN 0733-9399/2004/4-451–458/$18.00.

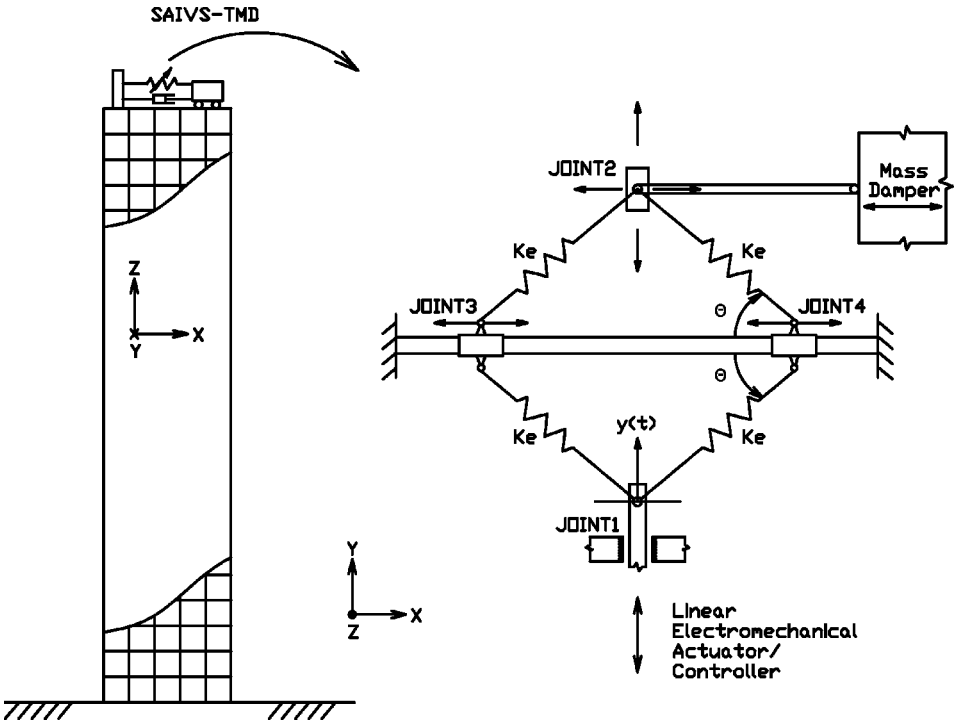

Fig. 1. Building with semiactive variable stiffness-tuned mass damper at the roof level and details of the semiactive variable stiffness device

trol algorithm developed by the writers. Detailed comparisons with a TMD and an ATMD with a linear quadratic Gaussian (LQG) controller developed by Yang et al. (2004) are presented. It is shown that SAIVS-TMD can reduce the response similar to that of an ATMD; however, with much less power consumption. It is shown that the SAIVS-TMD is very effective in reducing the response and is robust under building stiffness changes.

Semiactive Variable Stiffness Device and Semiactive Variable Stiffness-Tuned Mass Damper

Nagarajaiah [U.S. Patent No. 6,098,968 (2000)] has developed a new and innovative SAIVS device, which can change its stiffness continuously, independently, and smoothly between maximum and minimum stiffness. The SAIVS device consists of four spring elements arranged in a plane rhombus configuration with four pivot joints at the vertices as shown in Fig. 1. A linear electromechanical actuator configures the aspect ratio of the rhombus configuration of SAIVS device, under computer control. The aspect ratio changes between the fully closed (first diagonal between joints 1 and 2 being nearly zero) and open configurations (second diagonal between joints 3 and 4 being nearly zero) producing maximum and minimum stiffness, respectively. The control algorithm and controller are used to regulate the linear electromechanical actuator. The power required by the actuator to change the aspect ratio of the device is nominal. The variable stiffness of the SAIVS device can be described by the following equation:

$$K(t) = k_e \cos^2(\theta(t)) \tag{1}$$

where $K(t)$=time varying stiffness of the device; k_e=constant spring stiffness of each spring element; and $\theta(t)$=time varying angle of the spring elements with the horizontal in any position of the device as shown in Fig. 1.

The SAIVS device has maximum stiffness in its fully closed position $[\theta(t)=0]$ and minimum stiffness $[\theta(t)\sim\pi/2]$ in its fully open position (see Fig. 1). The device can be positioned in any configuration between the closed and open positions; thus, the device is capable of varying the stiffness continuously and smoothly between the maximum and minimum—the reader is referred to Nagarajaiah and Mate (1998), Nagarajaiah [U.S. Patent No. 6,098,969 (2000)], Spencer and Nagarajaiah (2003) for force–displacement loops showing the continuous variation of stiffness from maximum to minimum. The SAIVS device has been tested and shown to be effective by Nagarajaiah and Mate (1998) and Nagarajaiah and Varadarajan (1999).

The SAIVS-TMD has been developed by Nagarajaiah and Varadarajan (2000), based on SAIVS device, and studied using a three-story scaled model both analytically and experimentally. The SAIVS-TMD consists of the SAIVS device attached to a mass damper as shown in Fig. 1. The tuning is accomplished by varying the stiffness of the TMD continuously with real time control using the SAIVS device. Nagarajaiah and Varadarajan (2000) have developed the HT instantaneous frequency control algorithm and shown its effectiveness analytically and experimentally. In this paper, the newly developed SAIVS-TMD and the EMD and HT algorithm are applied for vibration control of a wind excited tall benchmark building.

Analytical Modeling

A detailed time varying analytical model is developed with a linear time invariant primary system and time variant SAIVS-TMD system. The SAIVS-TMD with a mass of 500 tons (mass ratio=0.327% with respect to the total mass of the building), similar to the TMD and ATMD, is considered. The first five natural frequencies of the primary structure are 0.16, 0.765, 1.992, 3.79, and 6.395 Hz; the corresponding damping ratio of the modes is 1%. In order to evaluate the robustness of the controller, a stiffness uncertainty of ±15% is considered. The building fundamental frequency is 0.172 Hz in the +15% case and 0.148 Hz

in the −15% case. The frequency of the SAIVS-TMD can vary between 0.148 to 0.172 Hz. The damping ratio of the SAIVS-TMD is chosen to be 7% for optimal response reduction. To save computational effort reduced-order 24 degrees of freedom (DOF) model is used. The first 48 complex modes are used in the model. The state space model of the system is as follows:

$$\dot{\mathbf{X}}(t)=\mathbf{A}(t)\mathbf{X}(t)+\mathbf{E}\mathbf{w}(t) \tag{2}$$

$$Y(t)=\mathbf{C}\mathbf{X}(t)+v(t) \tag{3}$$

with $X=(x,\dot{x})$, where x includes the displacements at the reduced-order 23 DOF; and x_m=the TMD displacement; all with respect to the ground, $Y(t)$=76th floor displacement. $\mathbf{w}$=the excitation and v=measured noise. The specified nondimensional performance criteria (Yang et al. 2004) are used for comparisons and evaluation of the response. Values of less than 1.0 for each performance criterion means a reduction in the response in the case with control when compared to the uncontrolled case, except for performance indexes J_5, J_6, J_{11}, and J_{12}. For further details of these criteria, the reader is referred to Yang et al. (2004).

Empirical Mode Decomposition and Hilbert Transform Algorithm

The EMD technique, developed by Haung et al. (1998), adaptively decomposes a signal into ''intrinsic mode functions'' (IMFs) that admit a well-behaved HT. The time–frequency representation is extracted from the decomposition, using the Hilbert amplitude spectrum. The principal technique is to decompose a signal into a sum of functions that: (1) have the same numbers of zero crossings and extrema, and (2) are symmetric with respect to the local mean. The first condition is similar to the narrow-band requirement for a stationary Gaussian process. The second condition modifies a global requirement to a local one, and is necessary to ensure that the instantaneous frequency will not have unwanted fluctuations as induced by asymmetric wave forms. These functions are called intrinsic mode functions (denoted by IMF_i or $\overline{x_i}$) obtained iteratively (Haung et al. 1998). The jth DOF displacement, $x_j(t)$, can be decomposed as follows:

$$x_j(t)=\sum_{i=1}^{n}\text{IMF}_i(t)+r_n(t)=\sum_{i=1}^{n}\overline{x_i}(t)+r_n(t) \tag{4}$$

where $r_n(t)$=residue of the decomposition. The intrinsic mode functions are obtained using the following algorithm:

1. Initialize; $r_0=\overline{x}(t)$, $i=1$.
2. Extract the IMF_i as follows:
   - Initialize: $h_0(t)=r_{i-1}(t)$, $j=1$.
   - Extract the local minima and maxima of $h_{j-1}(t)$.
   - Interpolate the local maxima and the local minima by a spline to form upper and lower envelopes of $h_{j-1}(t)$.
   - Calculate the mean m_{j-1} of the upper and lower envelopes.
   - $h_j(t)=h_{j-1}(t)-m_{j-1}(t)$.
   - If the stopping criterion is satisfied, then set $\text{IMF}_i(t)=h_j(t)$ or go to the extraction of the local minima and maxima of $h_{j-1}(t)$ with $j=j+1$.
3. $r_i(t)=r_{i-1}(t)-\text{IMF}_i(t)$.
4. If $r_i(t)$ still has at least two extrema then go to step 2 with $i=i+1$ or the decomposition is finished and $r_i(t)$ is the residue.

The analytical signal, $y_i(t)$, associated with each $\text{IMF}_i(t)$ or $\overline{x_i}(t)$ component can be obtained as follows:

$$\overline{x_i}(\omega)=\frac{1}{\sqrt{2\pi}}\int_{-\infty}^{\infty}\overline{x_i}(t)e^{-j\omega t}dt \tag{5}$$

$$y_i(t)=2\frac{1}{\sqrt{2\pi}}\int_0^{\infty}\overline{x_i}(\omega)e^{j\omega t}d\omega=\frac{1}{\pi}\int_0^{\infty}\int_{-\infty}^{\infty}\overline{x_i}(\tau)e^{j\omega(t-\tau)}d\tau d\omega \tag{6}$$

$$y_i(t)=\overline{x_i}(t)+\frac{j}{\pi}\int_{-\infty}^{\infty}\frac{\overline{x_i}(\tau)}{t-\tau}d\tau \tag{7}$$

where the HT

$$H[\overline{x}(t)]=\frac{1}{\pi}\int_{-\infty}^{\infty}\frac{\overline{x_i}(\tau)}{t-\tau}d\tau \tag{8}$$

hence

$$y_i(t)=\overline{x_i}(t)+jH[\overline{x_i}(t)]=\overline{x_i}(t)+j\tilde{x}_i(t) \tag{9}$$

As per Eq. (6) and Cohen (1995), the analytic signal can also be obtained by: (1) taking the Fourier transform of $\overline{x_i}(t)$; (2) zeroing the amplitude for negative frequencies and doubling the amplitude for positive frequencies; and (3) taking the inverse Fourier transform. The analytic signal $y_i(t)$ can also be expressed as

$$y_i(t)=A_i(t)e^{j\theta_i t} \tag{10}$$

where $A_i(t)$=instantaneous amplitude; and $\theta_i(t)$=instantaneous phase

$$A_i(t)=\sqrt{\overline{x_i}^2(t)+\tilde{x}_i^2(t)} \tag{11}$$

$$\theta_i(t)=\arctan\left(\frac{\tilde{x}_i(t)}{\overline{x_i}(t)}\right) \tag{12}$$

The instantaneous frequency (Cohen 1995), corresponding to an $\text{IMF}_i(t)$ or $\overline{x_i}$, is given by

$$f_i(t)=\frac{1}{2\pi}\frac{d\theta_i(t)}{dt} \tag{13}$$

Empirical Mode Decomposition/Hilbert Transform Instantaneous Frequency Control Algorithm

The stiffness of the SAIVS device is varied continuously to tune the SAIVS-TMD. The instantaneous frequency is identified based on empirical mode decomposition and Hilbert transform [Eqs. (4)–(13)] algorithm. The displacement of the 76th floor is the only feedback used in the instantaneous frequency algorithm. Once the dominant instantaneous frequency at which the structure is responding is identified, the stiffness of the SAIVS-TMD is adapted to tune and maximize the response reduction. The normalized top floor displacement frequency response curves—normalized with respect to static displacement—considering only the first mode and 1% modal damping, for the cases with 0 and ±15% stiffness uncertainty are shown in Fig. 2. For the wind response computations, all modes are considered. The first mode frequency of the primary structure is 0.16, 0.148, and 0.172 Hz for the case with 0 and ±15% stiffness uncertainty, respectively. The TMD is optimally tuned at 0.16 Hz for 0% stiffness uncertainty and maintained at originally tuned 0.16 Hz for ±15% stiffness uncertainty; however, the SAIVS-TMD is retuned in the frequency range of 0.148 to 0.172 Hz. For 0% damping in the TMD case, the two resonant peaks occur at frequencies ~0.155 and ~0.165 Hz. As the damping in the TMD case increases to 7 and 20% a single resonant peak occurs at frequency ~0.16 Hz as shown in Fig. 2; the corresponding resonant peak occurs at

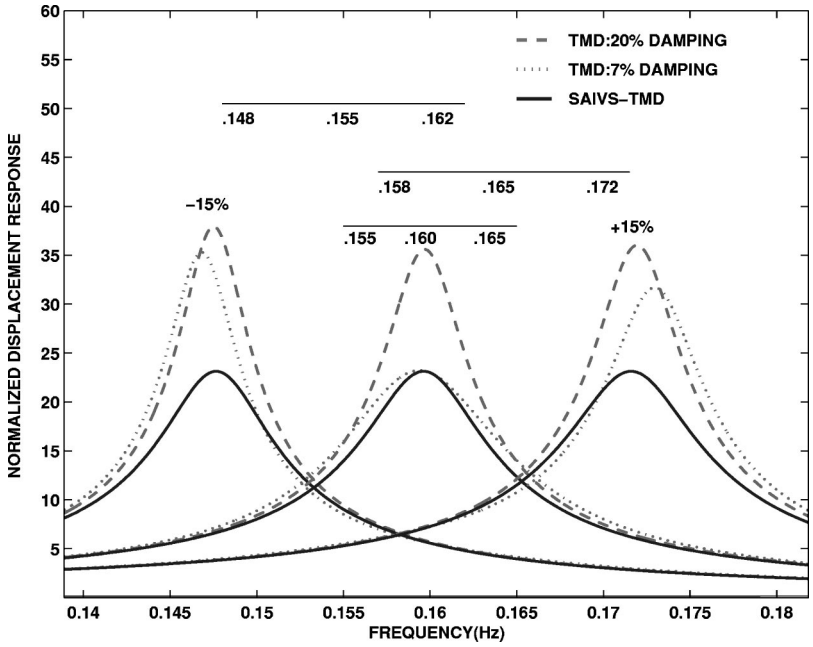

Fig. 2. Normalized top floor displacement frequency response curves for the case with −15, 0, and 15% uncertainty

~0.148 and ~0.172 Hz in the −15 and +15% stiffness uncertainty case, respectively. The tuning frequency ranges for the EMD/HT algorithm are chosen based on the frequency response curves, shown in Fig. 2, to ensure optimal response reduction. In Figs. 2 and 4, the first range spans from 0.148 to 0.162 Hz, covering the response peaks in the case of −15 and 0% stiffness uncertainty, with a central frequency of 0.155 Hz. The second range spans 0.158 to 0.172 Hz, covering the response peaks in the case of 0 and +15% stiffness uncertainty, with a central frequency of 0.165 Hz. The third range spans from 0.155 to 0.165 Hz—two resonant frequencies for 0% damping and the central frequencies of the first and second range—covering the response peak in the case of 0% stiffness uncertainty, with a central frequency of 0.16 Hz. The overlap of the three frequency ranges spans from 0.158 to 0.162 Hz—the range in which there is significant differences in response between the TMD (with 20% damping) and SAIVS-TMD cases. As is evident, generally, the frequency ranges for the EMD/HT algorithm can be arrived at based on the resonant frequencies for the original structure (without stiffness uncertainty) with an optimally tuned TMD, the frequencies of the structure with stiffness uncertainty, and the corresponding frequency response curves.

The EMD/HT control algorithm developed, shown in Figs. 3 and 4, is as follows:

1. A moving window of 3,072 time steps, $\Delta t = 0.01$ s, or 30.72 s is chosen to determine the EMD intrinsic mode components, IMF_i, from the 76th floor displacement; only the first two components, $\mathrm{IMF}_{1,2}$, are used, since they represent the first two dominant instantaneous frequencies of the structure with SAIVS-TMD.
2. The instantaneous frequency of each component, $\mathrm{IMF}_{1,2}$, is identified and updated at every $\Delta t_{\mathrm{EMD}} = 0.1$ s using the HT, Eqs. (8) and (13).
3. The dominant frequency, f_d, in each window is identified from $\mathrm{IMF}_{1,2}$. If f_d is greater than 0.172 Hz then it is reset to 0.172 Hz; if f_d is less than 0.148 Hz, then it is reset to 0.148 Hz; and if it is between 0.148 and 0.172 Hz, then it reset to 0.16 Hz—this is needed to maintain a reasonable running average frequency.
4. f_d is then used for computing the running average frequency, f_{avg} as shown in Fig. 4.
5. If the $f_{\mathrm{avg}} < 0.15$ Hz, the SAIVS stiffness is chosen such that the SAIVS-TMD frequency is either 0.148 or 0.155 or 0.162 Hz, as shown in Fig. 4, based on the value of f_d.
6. If the $f_{\mathrm{avg}} > 0.165$ Hz the SAIVS stiffness is chosen such that the SAIVS-TMD frequency is either 0.158 or 0.165 or 0.172 Hz, as shown in Fig. 4, based on the value of f_d.
7. If the $f_{\mathrm{avg}} \geqslant 0.15$ Hz or $f_{\mathrm{avg}} \leqslant 0.165$ Hz, the SAIVS stiffness is chosen such that the SAIVS-TMD frequency is either 0.155 Hz or 0.16 Hz or 0.165 Hz, as shown in Fig. 4, based on the value of f_d.

Results

In the frequency response curves shown in Fig. 2, TMD and SAIVS-TMD are equally effective for 0% stiffness uncertainty;

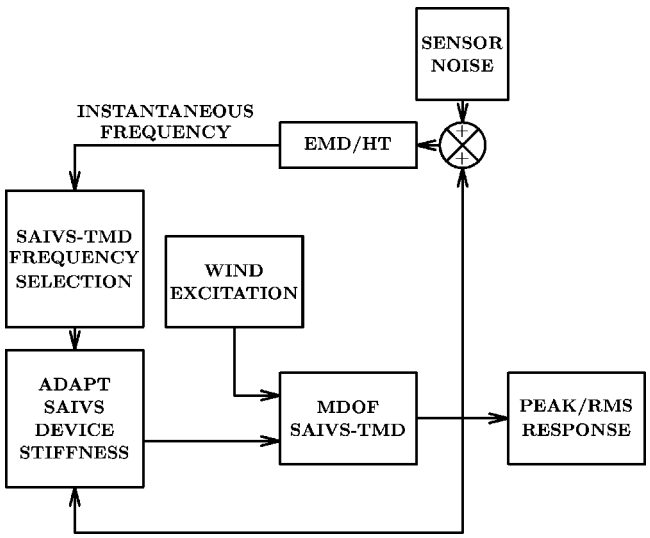

Fig. 3. Empirical mode decomposition/Hilbert transform control algorithm for adapting semiactive variable stiffness-tuned mass damper instantaneous frequency and stiffness

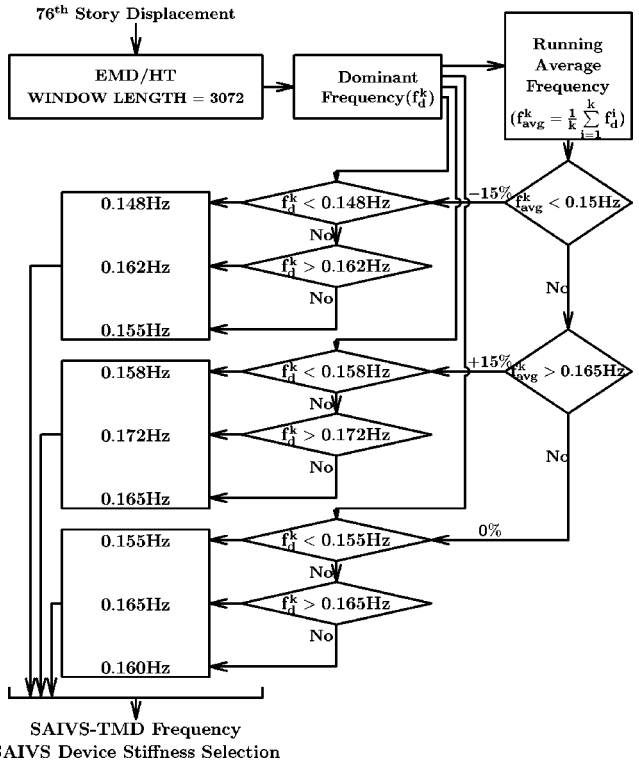

Fig. 4. Selection of semiactive variable stiffness-tuned mass damper instantaneous frequency and stiffness based on feedback and empirical mode decomposition/Hilbert transform algorithm

although, SAIVS-TMD reduces the response slightly more than the TMD, the differences are not significant. However, as is evident in Fig. 2, in the cases with ±15% stiffness uncertainty, the SAIVS-TMD proves to be clearly more effective in reducing the response—with reductions of up to 35%—due to its distinct advantage of retuning.

The computed response, for 0 and ±15% stiffness uncertainty, to wind excitation is presented in detail; the comparisons between the displacement and acceleration response of TMD, ATMD, and SAIVS-TMD are presented. The responses of the TMD computed

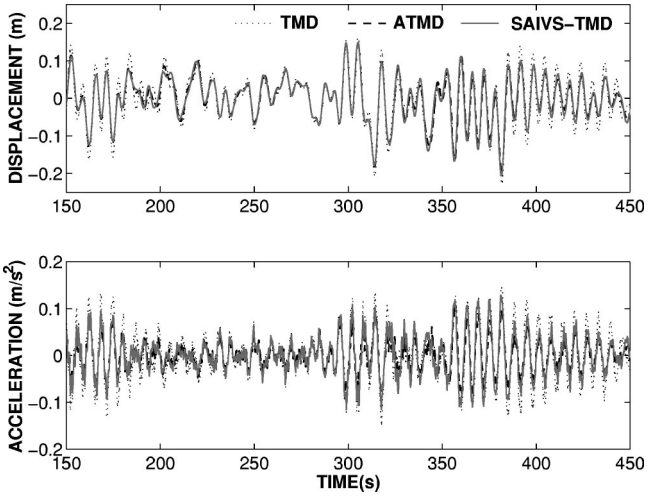

Fig. 5. Comparison of displacement and acceleration response of the 75th floor for 0% stiffness uncertainty

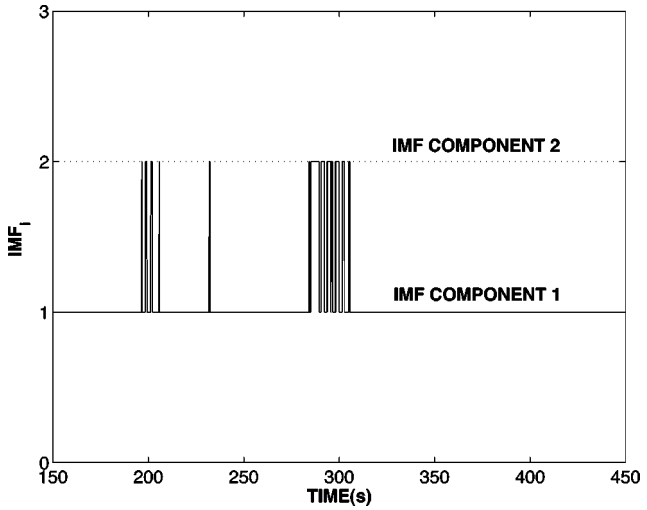

Fig. 6. Intrinsic mode function components used for stiffness adaptation of the semiactive variable stiffness device in the semiactive variable stiffness-tuned mass damper

and presented in this study are identical to that of Yang et al. (2004). The ATMD is controlled by a LQG controller developed by Yang et al. (2004); all the ATMD results presented in this study are from Yang et al. (2004).

The computed displacement and acceleration response for 0% stiffness uncertainty is shown in Fig. 5, for the three cases with TMD, SAIVS-TMD, and ATMD. The responses of the SAIVS-TMD and ATMD are comparable and are less than the response of the TMD. The corresponding $IMF_{1,2}$ components are shown in Fig. 6; the dominant component is used in selection of the SAIVS-TMD frequency as shown in Fig. 4. The force–displacement response of the TMD spring and SAIVS device of the SAIVS-TMD are shown in Fig. 7. The stiffness variation, evident in Fig. 7, in the case of SAIVS-TMD, tunes the frequency continuously to achieve maximum reduction in response, whereas, the stiffness of the TMD remains fixed. From the 75th floor acceleration power spectral density for TMD, SAIVS-TMD,

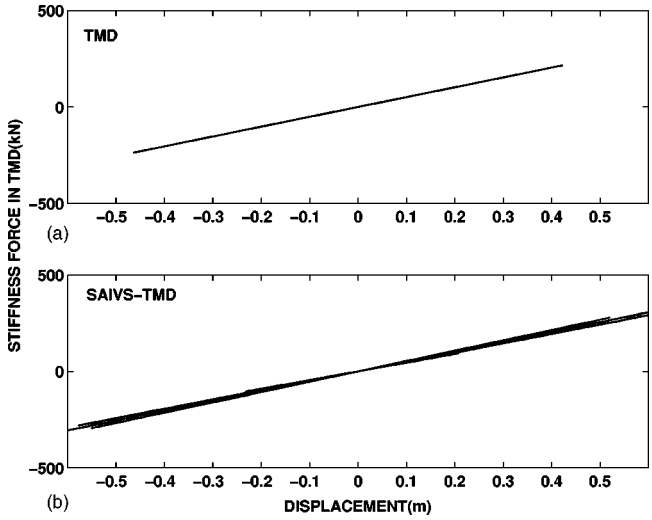

Fig. 7. Force–displacement behavior: (a) Tuned mass damper spring and (b) semiactive variable stiffness-tuned mass damper variable stiffness spring

Table 1. Comparison of Peak Response for 0% Uncertainty in Stiffness

Floor No.	Uncontrolled x_{pio} (cm)	Uncontrolled $\ddot{x}_{pio}$ (cm/s^2)	Tuned mass damper x_{pi} (cm)	Tuned mass damper $\ddot{x}_{pi}$ (cm/s^2)	Active tuned mass damper[a] x_{pi} (cm)	Active tuned mass damper[a] $\ddot{x}_{pi}$ (cm/s^2)	Semiactive variable stiffness-tuned mass damper x_{pi} (cm)	Semiactive variable stiffness-tuned mass damper $\ddot{x}_{pi}$ (cm/s^2)
1	0.05	0.22	0.04	0.21	0.04	0.23	0.04	0.27
30	6.84	7.14	5.60	4.68	5.14	3.37	5.11	3.91
50	16.59	14.96	13.34	9.28	12.22	6.73	12.14	7.54
55	19.41	17.48	15.54	10.74	14.22	8.05	14.13	8.25
60	22.34	19.95	17.80	12.69	16.27	8.93	16.17	8.86
65	25.35	22.58	20.10	14.72	18.36	10.05	18.25	10.37
70	28.41	26.04	22.43	16.77	20.48	10.67	20.35	11.75
75	31.59	30.33	24.84	19.79	22.67	11.56	22.52	14.02
76	32.30	31.17	25.38	20.52	23.15	15.89	23.01	14.68
Md	—	—	42.36	46.18	74.27	72.74	68.01	69.37

[a]Response of the active tuned mass damper baseline linear quadratic Gaussian controller from Yang et al. (2004).

Table 2. Comparison of Root-Mean-Square Response for 0% Uncertainty in Stiffness

Floor No.	Uncontrolled σ_{pio} (cm)	Uncontrolled $\ddot{\sigma}_{pio}$ (cm/s^2)	Tuned mass damper σ_{pi} (cm)	Tuned mass damper $\ddot{\sigma}_{pi}$ (cm/s^2)	Active tuned mass damper[a] σ_{pi} (cm)	Active tuned mass damper[a] $\ddot{\sigma}_{pi}$ (cm/s^2)	Semiactive variable stiffness-tuned mass damper σ_{pi} (cm)	Semiactive variable stiffness-tuned mass damper $\ddot{\sigma}_{pi}$ (cm/s^2)
1	0.02	0.06	0.01	0.06	0.01	0.06	0.01	0.06
30	2.15	2.02	1.48	1.23	1.26	0.89	1.29	0.99
50	5.22	4.78	3.57	2.80	3.04	2.03	3.10	2.17
55	6.11	5.59	4.17	3.26	3.55	2.41	3.63	2.52
60	7.02	6.42	4.79	3.72	4.08	2.81	4.16	2.88
65	7.97	7.31	5.43	4.25	4.62	3.16	4.72	3.30
70	8.92	8.18	6.08	4.76	5.17	3.38	5.28	3.69
75	9.92	9.14	6.75	5.38	5.74	3.34	5.86	4.19
76	10.14	9.35	6.90	5.48	5.86	4.70	5.99	4.28
Md	—	—	12.76	13.86	23.03	22.40	22.37	22.81

[a]Response of active tuned mass damper baseline linear quadratic Gaussian controller from Yang et al. (2004).

and ATMD (not shown due to space limitations) it is found that the SAIVS-TMD reduces the response in the first mode and as well as in the higher modes.

The simulation results are presented in Tables 1 through 5. Table 1 compares the peak displacement and acceleration responses of the uncontrolled structure, the structure with TMD, the structure with SAIVS-TMD, and the structure with ATMD, in the case with 0% stiffness uncertainty. The TMD reduces the 76th floor displacement and acceleration response by 21 and 34%, respectively, when compared to the uncontrolled case. From Table 1, it is evident that the SAIVS-TMD reduces the peak displacement and acceleration response of the 76th floor by 32 and 53%, respectively, when compared to the uncontrolled case; corresponding reductions in the case of ATMD are 28 and 49%, respectively. A further reduction in the case of SAIVS-TMD, when compared to the TMD case, is 10% response reduction in displacement and 29% response reduction in acceleration; the corresponding reductions in the case of ATMD are 9 and 23%. Hence, it is evident that SAIVS-TMD is as effective as ATMD in reducing the response. In the case of transient response to wind excitation, SAIVS-TMD is more effective than the TMD (even though the TMD is tuned in the case with 0% stiffness uncertainty) due to its distinct advantage of retuning—unlike the harmonic response, where both cases are equally effective as shown in Fig. 2.

The root-mean-square (rms) displacement and acceleration responses are compared for the same cases in Table 2. The reductions in the 76th floor displacement and acceleration RMS response are nearly 40 and 54%, respectively, in the case of SAIVS-TMD, when compared to the uncontrolled case; similar reductions are observed in the case of ATMD also. The 76th floor displacement and acceleration responses are further reduced by 13 and 22%, respectively, in the case of SAIVS-TMD, when compared to the TMD case.

In Table 3, the performance criteria J_1 through J_{12} are presented for SAIVS-TMD and ATMD cases for stiffness uncertainty, $\Delta K=0$, and $\pm 15\%$. Similar performances in the SAIVS-TMD and ATMD cases are evident in Table 3. A nearly 50% reduction occurs in the rms acceleration criteria, J_1 and J_2, peak acceleration criteria, J_7 and J_8. The reduction in the rms dis-

Table 3. Comparison of Performance Criteria

Root-mean-square responses semiactive variable stiffness-tuned mass damper[a]				Peak responses semiactive variable stiffness-tuned mass damper[a]			
Criteria	$\Delta K=0\%$	$\Delta K=15\%$	$\Delta K=-15\%$	Criteria	$\Delta K=0\%$	$\Delta K=15\%$	$\Delta K=-15\%$
J_1	0.458	0.458	0.504	J_7	0.462	0.500	0.569
	(0.369)	(0.365)	(0.387)		(0.381)	(0.411)	(0.488)
J_2	0.452	0.448	0.495	J_8	0.465	0.476	0.564
	(0.417)	(0.409)	(0.438)		(0.432)	(0.443)	(0.539)
J_3	0.591	0.506	0.737	J_9	0.712	0.619	0.827
	(0.578)	(0.487)	(0.711)		(0.717)	(0.607)	(0.770)
J_4	0.592	0.507	0.738	J_{10}	0.721	0.627	0.835
	(0.580)	(0.489)	(0.712)		(0.725)	(0.614)	(0.779)
J_5	2.206	1.788	2.441	J_{11}	2.105	1.814	2.553
	(2.271)	(1.812)	(2.709)		(2.300)	(1.852)	(2.836)
J_6	2.378	2.079	2.464	J_{12}	2.274	2.107	2.594
	(11.99)	(8.463)	(16.61)		(71.87)	(52.68)	(118.33)

[a]Response of the active tuned mass damper baseline linear quadratic Gaussian controller from Yang et al. (2004).

Table 4. Comparison of Peak Response for +15% Uncertainty in Stiffness

Floor No.	Uncontrolled		Tuned mass damper		Active tuned mass damper[a]		Semiactive variable stiffness-tuned mass damper	
	x_{pio} (cm)	$\ddot{x}_{pio}$ (cm/s^2)	x_{pi} (cm)	$\ddot{x}_{pi}$ (cm/s^2)	x_{pi} (cm)	$\ddot{x}_{pi}$ (cm/s^2)	x_{pi} (cm)	$\ddot{x}_{pi}$ (cm/s^2)
1	0.04	0.22	0.03	0.22	0.03	0.23	0.04	0.30
30	5.52	4.78	4.40	4.38	4.35	3.36	4.44	3.97
50	13.37	11.28	10.65	8.16	10.35	6.63	10.55	7.12
55	15.63	12.85	12.43	9.67	12.04	8.00	12.28	8.12
60	17.94	14.91	14.27	11.18	13.78	9.13	14.06	9.11
65	20.32	16.87	16.15	12.79	15.55	10.09	15.87	10.53
70	22.72	18.98	18.05	14.57	17.34	11.58	17.69	12.81
75	25.20	21.75	20.01	16.86	19.19	12.46	19.58	15.15
76	25.76	21.60	20.45	16.84	19.60	15.86	19.98	15.69
Md	—	—	32.61	35.73	59.83	60.87	58.58	59.83

[a]Response of the active tuned mass damper baseline linear quadratic Gaussian controller from Yang et al. (2004).

placement criteria, J_3 and J_4, peak displacement criteria, J_9 and J_{10} varies from 15 to 50%. The performance in the case of SAIVS-TMD is nearly the same as the ATMD. However, the important difference in the case of SAIVS-TMD, is J_6—the average power consumption—being significantly smaller, and J_{12}—the peak power consumption—being an order of magnitude smaller, when compared to the ATMD. Fully active systems need substantial power since they apply active forces onto the ATMD. However, the SAIVS-TMD reduces the response due to continuous variation of stiffness and retuning of the frequency and not by application of active forces; thus, the semiactive case needs nominal power. Also, in the event of power failure, the SAIVS-TMD can act as a TMD and still be effective.

Table 4 presents the peak displacement and acceleration responses for uncontrolled, TMD, ATMD, and SAIVS-TMD cases for stiffness uncertainty of +15%. The TMD reduces the 76th floor displacement and acceleration response by nearly 20%, when compared to the uncontrolled case; the corresponding reductions in the case of SAIVS-TMD and ATMD are nearly 25%. The displacement response reduction of 0 to 5% occurs in the ATMD and SAIVS-TMD cases compared to the TMD case. The acceleration response reduction of 5 to 10% occurs in the ATMD and SAIVS-TMD cases compared to the TMD case; it should be kept in mind that SAIVS-TMD power requirements are substantially lower than that of the ATMD.

Table 5 presents the peak displacement and acceleration responses for uncontrolled, TMD, ATMD, and SAIVS-TMD cases for stiffness uncertainty values of −15%. The displacement and acceleration response for the case of TMD is within 5 to 10% of the uncontrolled case and clearly the effectiveness of the TMD is diminished since it is mistuned. However, the SAIVS-TMD is still effective as it can retune and reduce the response by nearly 25% when compared to the uncontrolled case, and by nearly 16% when compared to the TMD case. The responses of the SAIVS-TMD and the ATMD are within 5% of each other; it should be kept in mind that SAIVS-TMD power requirements are substantially lower than that of the ATMD. Hence, the SAIVS-TMD is effective is all cases, i.e., 0 and ±15% stiffness uncertainty, similar to an ATMD.

Conclusions

The effectiveness of SAIVS-TMD in response to the control of tall buildings has been studied and its performance evaluated analytically. The developed EMD/HT instantaneous frequency algo-

Table 5. Comparison of Peak Response for −15% Uncertainty in Stiffness

Floor No.	Uncontrolled		Tuned mass damper		Active tuned mass damper[a]		Semiactive variable stiffness-tuned mass damper	
	x_{pio} (cm)	$\ddot{x}_{pio}$ (cm/s^2)	x_{pi} (cm)	$\ddot{x}_{pi}$ (cm/s^2)	x_{pi} (cm)	$\ddot{x}_{pi}$ (cm/s^2)	x_{pi} (cm)	$\ddot{x}_{pi}$ (cm/s^2)
1	0.06	0.22	0.06	0.21	0.04	0.22	0.05	0.21
30	7.69	6.01	7.91	5.08	5.54	3.64	5.91	4.04
50	18.34	12.83	16.92	10.93	13.12	7.87	14.03	8.39
55	21.37	14.41	19.72	12.26	15.27	9.90	16.34	9.97
60	24.49	15.97	22.59	13.63	17.47	11.13	18.71	11.10
65	27.68	17.40	25.53	15.39	19.72	12.63	21.13	12.80
70	30.90	19.86	28.50	17.95	21.99	14.01	23.59	14.64
75	34.24	23.09	31.58	21.08	24.34	14.80	26.13	17.27
76	34.99	22.80	32.27	20.73	24.87	18.76	26.70	17.39
Md	—	—	44.93	48.65	91.60	79.06	82.46	77.49

[a]Response of active tuned mass damper baseline linear quadratic Gaussian controller from Yang et al. (2004).

rithm is effective in identifying the dominant frequency and in the selection of the stiffness to reduce the response to wind excitation. The results confirm the robust performance of the SAIVS-TMD in reducing the response of tall structures, even in cases with $\pm 15\%$ stiffness uncertainty. The TMD loses its effectiveness with 15% stiffness variation. The SAIVS-TMD can reduce the response similar to that of an ATMD; however, with an order of magnitude less power consumption.

Acknowledgments

Funding for this project provided by the National Science Foundation, NSF Career Grant CMS-9996244, is gratefully acknowledged.

References

Abe, M., and Fujino, Y. (1994). ''Dynamic characterization of multiple tuned mass dampers and some design formulas.'' *Earthquake Eng. Struct. Dyn.*, 23, 813–835.

Abe, M., and Igusa, T. (1996). ''Semi-active dynamic vibration absorbers for controlling transient response.'' *J. Sound Vib.*, 198(5), 547–569.

Bobrow, J., Jabbari, F., and Thai, K. (2000). ''A new approach to shock isolation and vibration suppression using a resetable actuator.'' *J. Dyn. Syst., Meas., Control*, 122, 570–573.

Cohen, L. (1995). *Time–frequency analysis*, 1st Ed., Prentice-Hall, New Jersey.

Den Hartog, J. P. (1947). *Mechanical vibrations*, McGraw-Hill, New York.

Gavin, H. (1998). ''Design method for high-force electrorheological dampers.'' *Smart Mater. Struct.*, 7, 664–673.

Haung, E. N., et al. (1998). ''The empirical mode decomposition and the Hilbert spectrum for nonlinear and nonstationary time series analysis.'' *Proc. R. Soc. London, Ser. A*, 454, 903–995.

Hrovat, D., Barak, P., and Rabins, M. (1983). ''Semiactive versus passive or active tuned mass dampers for structural control.'' *J. Eng. Mech.*, 109(3), 691–705.

Igusa, T., and Xu, K. (1992). ''Dynamic characteristics of multiple tuned mass substructures with closed spaced frequencies.'' *Earthquake Eng. Struct. Dyn.*, 21, 1050–1070.

Ikeda, Y., Sasaki, K., Sakamoto, M., and Kobori, T. (2001). ''Active mass driver system as the first application of active structural control.'' *Earthquake Eng. Struct. Dyn.*, 30(11), 1575–1595.

Kareem, A., and Kline, S. (1995). ''Performance of multiple mass dampers under random loading.'' *J. Struct. Eng.*, 121(2), 348–361.

Kobori, T., and Takahashi, M. (1993). ''Seismic response controlled structure with active variable stiffness system.'' *Earthquake Eng. Struct. Dyn.*, 22(12), 925–941.

Kurata, N., Kobori, T., Takahashi, M., Niwa, N., and Midorikawa, H. (1999). ''Actual seismic response controlled building with semiactive damper system.'' *Earthquake Eng. Struct. Dyn.*, 28, 1427–1447.

Nagarajaiah, S., and Mate, D. (1998). ''Semiactive control of continuously variable stiffness system.'' *Proc., 2nd World Conf. Struct. Control*, Vol. 1, Kyoto, Japan, 397–405.

Nagarajaiah, S., and Varadarajan, N. (2000). ''Novel semiactive variable stiffness tuned mass damper with real time tuning capability.'' *Proc., 13th Engineering Mechanics Conf.* (CD-ROM), ASCE, Reston, Va.

Nagarajaiah, S., Varadarajan, N., and Sahasrabudhe, S. (1999). ''Variable stiffness and instantaneous frequency.'' *Proc., World Structures Congress*, ASCE, Reston, Va., 858–861.

Nasu, T., Kobori, T., Takahashi, M., Niwa, J., and Ogasawara, K. (2001). ''Active variable stiffness system with non-resonant control.'' *Earthquake Eng. Struct. Dyn.*, 30(10), 1597–1614.

Reinhorn, A., et al. (1993). ''Full-sale implementation of active control. II: Installation and performance.'' *J. Struct. Eng.*, 119(6), 1935–1960.

Soong, T. T. (1990). *Active structural control: Theory and practice*, Longman, New York.

Spencer, B. F., Dyke, S. J., Sain, M. K., and Carlson, J. D. (1997). ''Phenomenological model for magnetorheological dampers.'' *J. Eng. Mech.*, 123(3), 230–238.

Spencer, B. F., and Nagarajaiah, S. (2003). ''State of the art of structural control.'' *J. Struct. Eng.*, 129(7), 1–10.

Symans, M., and Constantinou, M. C. (1999). ''Seismic testing of a building structure with a semi-active fluid damper control system.'' *Earthquake Eng. Struct. Dyn.*, 26(7)21, 759–777.

Yang, J. N., Agrawal, A., Samali, B., and Wu, J. C. (2004). ''Benchmark problem for response control of wind-excited tall buildings.'' *J. Eng. Mech.*, 130(4), 437–446.

Yang, J. N., Kim, J. H., and Agrawal, A. (2000). ''Resetting semiactive stiffness damper for seismic response control.'' *J. Struct. Eng.*, 126(12), 1427–1433.